

ROSSI X-RAY TIMING EXPLORER ABSOLUTE TIMING RESULTS FOR THE PULSARS B1821–24 AND B1509–58

A. H. ROTS,^{1,2} K. JAHODA, AND D. J. MACOMB¹

Laboratory for High Energy Astrophysics, Code 660, NASA, Goddard Space Flight Center, Greenbelt, MD 20771; arots@head-cfa.harvard.edu

N. KAWAI

Institute of Physical and Chemical Research, Wako (RIKEN), Saitama 351-01, Japan

Y. SAITO

Institute of Space and Astronautical Science, Sagami-hara, Kanagawa 229, Japan

V. M. KASPI³

Department of Physics and Center for Space Research, Massachusetts Institute of Technology, Cambridge, MA 02139

A. G. LYNE

Department of Physics, University of Manchester, Jodrell Bank, Macclesfield, SK11 9DL, UK

R. N. MANCHESTER

Australia Telescope National Facility, CSIRO, P.O. Box 76, Epping, NSW 2121, Australia

D. C. BACKER AND A. L. SOMER

Astronomy Department and Radio Astronomy Laboratory, University of California, Berkeley, Berkeley, CA 94720

AND

D. MARSDEN AND R. E. ROTHSCHILD

Center for Astrophysics and Space Science, University of California, San Diego, San Diego, CA 92093

Received 1997 August 6; accepted 1998 February 19

ABSTRACT

Observations with the *Rossi X-Ray Timing Explorer* and the Jodrell Bank, Parkes, and Green Bank telescopes have enabled us to determine the time delay between radio and X-ray pulses in the two isolated pulsars B1821–24 and B1509–58. For the former we find that the narrow X-ray and radio pulse components are close to being coincident in time, with the radio peak leading by 0.02 period ($60 \pm 20 \mu\text{s}$), while the wide X-ray pulse component lags the last of the two wider radio components by about 0.08 period. For the latter pulsar we find, using the standard value for the dispersion measure, that the X-ray pulse lags the radio by about 0.27 period, with no evidence for any energy dependence in the range 2–100 keV. However, uncertainties in the history of the dispersion measure for this pulsar make a comparison to previous results difficult. It is clear that there are no perceptible variations in either the lag or the dispersion measure at timescales of a year or less.

Subject headings: ISM: general — pulsars: individual (PSR B1509–58, PSR B1821–24) — radio continuum: stars — X-rays: stars

1. INTRODUCTION

In the past, various attempts at absolute timing of pulsar signals have been made, in order to establish the phase lag between radio and X-ray pulses. Examples include the papers on PSR B1509–58 by Kawai et al. (1991) and Ulmer et al. (1993). From these we know that there is a phase lag and that it is, roughly speaking, between 0.25 and 0.35. First Buccheri et al. (1978) and, more recently, Kanbach et al. (1994) have measured the phase lag between gamma-ray and radio emission for the Vela pulsar. Masnou et al. (1994) reported for the Crab pulsar that the radio pulse appears to lag the gamma-ray pulse by about 0.5 ms, based on Figaro II observations. This was not confirmed by the *Compton Gamma Ray Observatory* (CGRO) observations of Nolan et al. (1993) and Ulmer et al. (1994) (respectively, EGRET and OSSE data), although the former did not comment on the issue. The latter find the phase lag

to be less than 30 μs , but with an uncertainty of 300 μs . Hence, we feel that it is fair to say that in the case of the Crab pulsar, for most past high-energy astrophysics space missions, the lag may be considered zero for all practical purposes because of uncertainties in absolute timekeeping. If there is a lag, it has to be significantly less than 1 ms.

This situation is different for the *Rossi X-Ray Timing Explorer* (RXTE or XTE) when using one or both of its main instruments, the proportional counter array (PCA) and the High-Energy X-Ray Timing Experiment (HEXTE). The precision and accuracy of the RXTE absolute timing will, in principle, allow measuring phase lags as short as 10 μs . This means that for all known X-ray pulsars the X-ray timekeeping will no longer be the dominant source of uncertainty. However, in most, if not all, cases we will not be able to achieve an accuracy of 10 μs since we will be limited by the accuracy of the radio observations, the differing shapes of the light curves (as well as variations therein depending on wave band and time), and counting statistics.

This type of measurement provides important information for a better understanding of the emission processes involved. In isolated neutron stars, powered by spin-down rather than accretion, the pulsed emission is likely to orig-

¹ Universities Space Research Association.

² Present address: Harvard-Smithsonian Center for Astrophysics, MS 81, 60 Garden Street, Cambridge, MA 02138.

³ Hubble Fellow.

inate from either a polar cap (Daugherty & Harding 1982) or synchrotron processes in the outer magnetospheric gaps (Cheng, Ho, & Ruderman 1986). For more quantitative treatment of the latter type of models see, e.g., Smith (1986), Romani & Yadigaroglu (1995). Accurate absolute timing data will increase our knowledge of the precise location where the emission originates and of the geometry of the magnetic field lines.

This paper presents absolute timing results for two stable radio pulsars, PSR B1821–24 and PSR B1509–58, by means of *RXTE* and the Jodrell Bank, Parkes, and Green Bank radio telescopes. For the former pulsar we will also make a comparison to *ASCA* observations. Together with similar results for the Crab pulsar (PSR B0531+21) that are described in a separate paper (Rots et al. 1998a, 1998b), the experiment demonstrates the capabilities of the *RXTE* in this area. In addition to the scientific results, it is our intention to provide with this paper a reference for *RXTE* absolute timing issues.

2. *RXTE* TIMING ACCURACY

The *RXTE* Mission Operations Center (MOC) performs about 10 calibration observations of the spacecraft clock per day. The calibration, by means of the User Spacecraft Clock Calibration System (USCCS; NASA/GSFC 1991) technique, relies on a round trip signal, tagged by the spacecraft clock's time stamp, to determine the spacecraft clock offset. The method claims to provide absolute time with an accuracy of 5 μ s. Parabolic fits to data sets extending over periods of about a week show deviations of no more than 1 μ s, which is consistent with quoted uncertainties for the various steps in the procedure. However, the true uncertainty is dominated by the clock at the ground station at White Sands, which is only "required to agree with UTC at the Naval Observatory to within 5000 ns (5 μ s)," although it "is typically kept within ... 2 μ s of UTC" (NASA/GSFC 1991). Consequently, we shall assume that *RXTE* absolute time is correct to within 5 μ s. In addition, however, most of the data used in the course of this investigation suffer from a slight additional degradation, leading us to adopt a value of 8 μ s for the uncertainty in absolute time for observations made before 1997 April 29 (MJD 50,567). This degradation was caused by a known error in the clock calibration ground software that was corrected on that date.

We have validated these calibrations by astronomical observations of burst source 1744–28 (comparing *CGRO-BATSE* and *RXTE*-PCA data) and the pulsars PSR B1509–58 (period 150 ms) and PSR B0531+21 (Crab, period 33 ms) to an accuracy of 1 ms. Beyond that level of accuracy, uncertainties in the knowledge of the properties of the celestial objects preclude further validation. However, the validation justifies, in our minds, accepting the MOC's calibration results.

All *XTE* data items are tagged with a time stamp taken from the spacecraft clock, with a maximum resolution of 1 μ s for PCA data, 8 μ s for HEXTE data. Measurements of timing delays internal in the spacecraft were made before launch by means of a muon source. These measurements compared the true time of the events to the time tags attached by the instrument data systems and hence include detector, as well as data system, delays. The timing delay for PCA events was determined to range from 16 μ s for most events to 20 μ s at low pulse heights, which is close to expected values. The delay is the sum of all analog pro-

cessing and transfer times, and the time tag is applied by the Experiment Data System (EDS). The HEXTE time stamp, on the other hand, is applied by the HEXTE data system at the moment the lower level discriminator is exceeded; the resulting HEXTE instrumental delay is less than 1 μ s.

The time, as recorded in *RXTE* FITS files is terrestrial time (TT), with an accuracy of better than 100 μ s. Additional corrections based on the MOC's calibrations can reduce the error to 8 μ s. The issue of time systems is dealt with in more detail in the *RXTE* guest observer facility World Wide Web pages⁴ (see "Time Tutorial"⁵ and "Absolute Time Calibration"⁶) and in full detail by Seidelmann, Guinot, & Doggett (1992).

All other sources of timing error that affect barycenter corrections are small compared to the clock uncertainties quoted above. The 3 σ errors for the solar system ephemeris and the *RXTE* orbit ephemeris are 0.1 μ s and 0.25 μ s, respectively. In summary, *RXTE* time stamps, with and without barycenter correction, can be corrected to within 5 μ s (8 μ s before MJD 50,567) of absolute time. We adopted corrections for the instrumental delays of 16 μ s and 1 μ s for PCA and HEXTE, respectively.

In this paper we present absolute timing results for two stable radio pulsars, PSR B1821–24 and PSR B1509–58. We do not include our extremely high signal-to-noise observations of the Crab pulsar here; interpretation of those data requires a careful treatment of the intrinsic timing noise in that source and will be reported separately (Rots et al. 1998).

3. ANALYSIS OF *RXTE* OBSERVATIONS

We report here on observations made with the two main instruments on *RXTE*. The PCA consists of five Xenon-filled detectors that cover the energy range 2–50 keV with a combined nominal collecting area of 7000 cm². HEXTE consists of two clusters of four NaI/CsI "phoswich" scintillation detectors that are usually rocking to provide a background estimate through a beam switching technique; the combined nominal collecting area is 800 cm² per cluster. Since we are interested in pulsed signals, we switched off the rocking.

Public *RXTE* observations of PSR B1821–24 were made on 1996 September 16 (MJD 50,342) in the context of an *RXTE*-*ASCA* clock cross calibration project. The total *RXTE* exposure time was 6559 s, divided over two orbits. The PCA data configuration used was *GoodXenon*, which records all good events detected in the Xenon chamber with full timing accuracy of 1 μ s. To improve the signal-to-noise ratio, we only used the photons detected in the top Xenon layer. The pulsed signal is too weak to be detected by HEXTE in such a short exposure. In this paper we will also present the *ASCA* observations that were made contemporaneously, as part of the cross calibration program. These observations are not the same as presented by Saito et al. (1997a), but are described in more detail by Saito et al. (1997b).

For PSR B1509–58, we present proprietary observations made with the PCA in the same *GoodXenon* data configuration, and HEXTE observations made with an

⁴ <http://rxte.gsfc.nasa.gov>.

⁵ http://heasarc.gsfc.nasa.gov/docs/xte/abc/time_tutorial.html.

⁶ <http://heasarc.gsfc.nasa.gov/docs/xte/abc/time.html>.

event data configuration with 8 μ s time resolution. These observations cover the period 1996 January through October.

The observations were analyzed by the program *faseBin*, developed by one of us (A. H. R.) and publicly distributed as part of the *Ftools* analysis package by the GSFC High-Energy Astrophysics Science Archive Research Center. The program selects only good events, calculates the absolute pulse phase, based upon the radio pulsar timing ephemeris, and bins the photon events in a two-dimensional histogram of energy channel versus pulse phase.

The time from the FITS files is corrected to 8 μ s accuracy and transformed from TT to barycentric dynamical time (TDB) by means of the *RXTE* orbit ephemeris and the JPL DE-200 solar system ephemeris (see Standish 1982, 1990). Both of these ephemerides are accurate to better than 1 μ s. The uncertainty introduced by the TDB-TT term is approximately 2 μ s. In summary, we feel confident that our time stamps are correct to 10 μ s. The same code and ephemeris are used to transform the timing ephemeris to TDB.

The two-dimensional histograms are then collapsed over one or more energy ranges to create light curves as a function of absolute phase, or over one or more phase ranges to allow phase-resolved spectroscopy. All X-ray pulse phases in this paper refer to the peak of the pulse. The timing ephemerides used are given in Table 1.

In the near future, we intend to switch the *faseBin* program from the DE-200 to the DE-405 ephemeris. At this place, for future reference, we shall briefly deal with the issues involved in that changeover. Aside from higher accuracy, there are two fundamental changes and two possible sources of inconsistencies. The two fundamental changes are as follows:

1. Although both ephemerides are based on the epoch J2000.0, DE-200 uses the older FK-5 reference system while DE-405 is tied to the International Celestial Reference System (ICRS), as adopted by the IAU at its 1997 General Assembly in Kyoto, Japan.

2. As a result of more accurate masses of the solar system bodies, the position of the barycenter has shifted. The difference can amount to several milliseconds.

In tying X-ray observations to radio timing ephemerides, the two potential inconsistencies, as it turns out, do in many cases not cause a problem.

1. The radio timing ephemerides, till the present, have been derived using DE-200. Fortunately, this cancels out

since the time of arrival of the pulse, or zero-phase (col. [5] in Table 1) is given in (i.e., converted back to) geocentric time, but only to the level of tens of microseconds. Hence, it cannot be ignored for millisecond pulsars. In the future radio ephemerides will be based on DE-405 and a code will be provided indicating which planetary ephemeris has been used.

2. The spacecraft orbit ephemeris may be (and usually is) provided in J2000.0 geocentric coordinates referenced to FK-5. The error incurred by adding such vectors to J2000.0 ICRS vectors is proportional to the length of the geocentric FK-5 vector. Since the misalignment between the two reference systems is about 20 milliarcseconds, the maximum error arising from this misalignment is approximately 2 ns times the distance of the spacecraft from the geocenter, expressed in Earth radii. Hence, the error is definitely negligible, not only for spacecraft in low Earth orbit like *RXTE*, but also for more elliptical orbits like *AXAF*.

4. PSR B1821–24

4.1. Comparison to Jodrell Bank and ASCA Observations

The timing ephemeris was derived from observations made with the Jodrell Bank Mark IA radio telescope, at an observing frequency of 1408 MHz, assuming a dispersion measure of 119.86 pc cm⁻³. The pulse profile, showing two pulse components, is included in Figure 1. In order to be consistent with the nomenclature in Backer & Sallmen (1997), we shall refer to the pulse component at phase 0.1 as number 2 and the one at phase 0.8 as number 1. The time resolution of the observations was about 300 μ s, or one-tenth of a period. The error in the determination of the dispersion measure leads to an uncertainty of about 150 μ s, or about 0.05 in phase, at infinite frequency. The timing ephemeris is labeled in Table 1 as B1821–24J. Note that the zero point of the phase of this ephemeris is different from that of the Green Bank ephemeris.

The *RXTE* signal-to-noise ratio is such that we only present one light curve: PCA 2–16 keV (channel 5–49). There are two clear peaks, a narrow one at phase 0.8 and an asymmetric one at phase 0.3, consistent with the separation between the peaks seen in the *ASCA* result reported by Saito et al. (1997a) but slightly offset in phase. The narrow pulse component has a width less than 0.04 in phase, corresponding to 100 μ s. Analysis of the two orbits separately shows that these two peaks are clearly present in both sets while all other features do not consistently appear in both;

TABLE 1
RADIO TIMING EPHEMERIDES

Pulsar (1)	R.A. (J2000.0) (2)	Decl. (J2000.0) (3)	MJD Range (4)	$t_{0,geo}$ (MJD [UTC]) (5)	$\dot{\nu}$ (s ⁻¹) (6)	$\ddot{\nu}$ (10 ⁻¹² s ⁻²) (7)	$\ddot{\nu}$ (10 ⁻²⁴ s ⁻³) (8)	rms ^a (9)
B1821–24J ^b	18 24 32.008	–24 52 11.12	50,059–50,372	50,215.000000023	327.4056597973296	–0.173520	0.0	22.2
B1821–24G ^c	18 24 32.008	–24 52 10.70	47,826–50,660	49,243.000000025	327.4056743697863	–0.173521	0.0581	6.8
B1509–58	15 13 55.627	–59 8 9.54	49,730–50,117	49,923.000000072	6.6284166684779	–67.4303	1990	8.8
B1509–58	15 13 55.627	–59 8 9.54	50,114–50,296	50,205.000000764	6.6267743270631	–67.3824	1950	9.1
B1509–58	15 13 55.627	–59 8 9.54	50,242–50,462	50,352.000000582	6.6259186740744	–67.3579	1950	8.0

NOTE.—Units of right ascension are hours, minutes, and seconds, and units of declination are degrees, arcminutes, and arcseconds.

^a In milliperiods.

^b Based on Jodrell Bank observations.

^c Based on Green Bank observations.

TABLE 2
PSR B1821L – 24 PULSE PEAK PHASES

Spectral Band	Timing Ephemeris	Pulse 1	Pulse 2	Pulse 3
X-ray (2–16 keV)	B1821–24J	0.775	...	0.31
Radio (Jodrell Bank, 1408 MHz)	B1821–24J	0.785	0.105	...
X-ray (2–16 keV)	B1821–24G	0.229 ± 0.003	...	0.77 ± 0.01
Radio (Green Bank, 800 MHz)	B1821–24G	0.209 ± 0.003	0.50 ± 0.01	0.69 ± 0.01

the latter must therefore be either spurious or time variable and will not be considered here.

We present the *RXTE* light curve in Figure 1, together with the *ASCA* Gas Imaging Spectrometer (GIS) and radio light curves. The background level (internal and cosmic background, and unpulsed source) is included. The total pulsed flux is about 1% of the combined unpulsed flux and backgrounds. These data prove that it is possible to detect with *RXTE* a narrow pulsed signal with a flux of only 0.5% of the unpulsed flux in a single orbit observation.

When the original *ASCA* observations were reported by Saito et al. (1997a), it was not at that time possible to

compare the *ASCA* and radio phases in an absolute sense, since the uncertainty in the *ASCA* clock was approximately 1 ms. This problem has been solved for the *ASCA* observations obtained in the context of the *RXTE-ASCA* clock cross calibration project that are presented in this paper. The uncertainty in the *ASCA* clock has been reduced to 200 μ s (see Saito et al. 1997b)⁷ and all phases in Figure 1 are calculated as absolute phases, applying all known clock corrections. The *ASCA* light curve exhibits the same features as the *RXTE* one, although they are shifted by approximately 0.05 period in phase ($\approx 150 \mu$ s). Errors of this magnitude have been observed in *ASCA*'s clock and attributed to drift due to temperature variations. Hence, we feel justified in assuming that *RXTE*'s absolute timing is the more correct one.

The phase information is summarized in Table 2. Note that this table uses the radio pulse component numbering from Backer & Sallmen (1997).

4.2. Comparison to Green Bank Observations

Recently, Backer & Sallmen (1997) published a new radio pulse profile of PSR B1821–24 based on observations made with the NRAO⁸ 42 m telescope at Green Bank, WV, at observing frequencies of 800 and 1395 MHz. Owing to the use of the Spectral Processor back end, the temporal resolution of the pulse profile is much higher than that of the Jodrell Bank one, revealing the existence of a third radio pulse component. Backer & Sallmen (1997) compared the result to *ASCA* observations, but no absolute phase comparison could be made. We have analyzed the *RXTE* observation using the timing ephemeris that was derived from the Green Bank observations (see Table 1, B1821–24G). The dispersion measure was, of course, determined for each observing session separately, based on the dual frequency data.

The resulting light curves, presented in Figure 2, are quite convincing. There is good agreement between the narrow X-ray pulse component and radio pulse component 1, as correctly anticipated by Backer & Sallmen (1997), but the broad X-ray pulse component lags radio component 3 by about 0.08 period. The X-ray version of pulse component 1 seems to lag the radio component by 60 μ s, which is not consistent with their being temporally coincident. The accuracy of the X-ray phase, 10 μ s (see § 3), is dominated by the uncertainty in the *RXTE* clock; the accuracy of the radio phase is approximately 10 μ s (1 σ), mainly due to uncer-

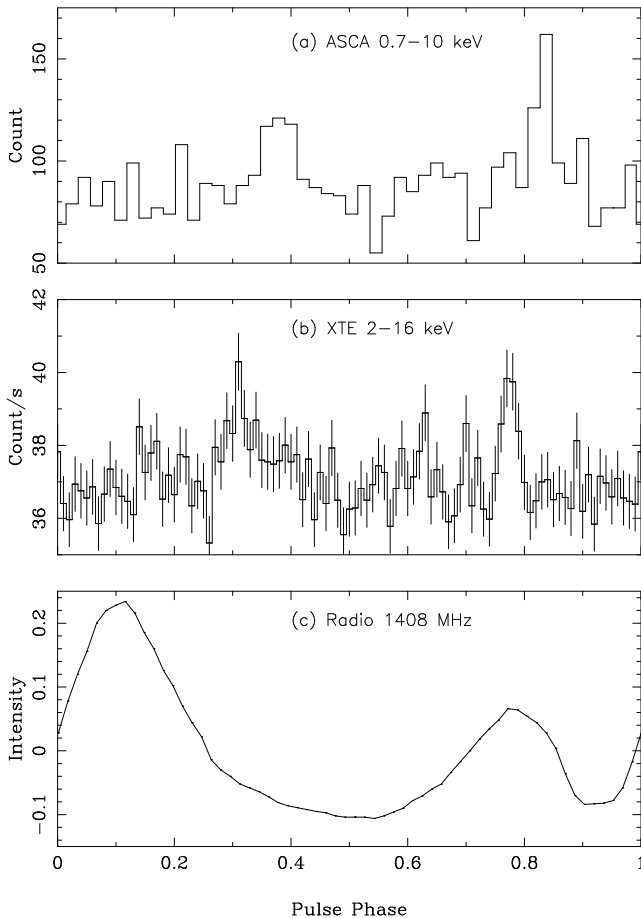


FIG. 1.—PSR B1821–24. Light curves based on (a) *ASCA* GIS (0.7–10 keV), (b) *RXTE* PCA (2–16 keV), (c) Jodrell Bank radio (1408 MHz) observations, using timing ephemeris B1821–24J. The *ASCA* light curve is labeled in total counts per bin (at 48 bins per period), the *RXTE* light curve in counts per second per bin (at 100 bins per period) with 1 σ errors indicated. The instrumental broadening in the radio profile amounts to about 0.1 in pulse phase. Note that the zero point of the phase of this ephemeris used in this figure is different from the one used in Fig. 2.

⁷ Also

http://heasarc.gsfc.nasa.gov/docs/asca/newsletters/gis_time_assign5.html.

⁸ The National Radio Astronomy Observatory is a facility of the National Science Foundation operated under cooperative agreement by Associated Universities, Inc.

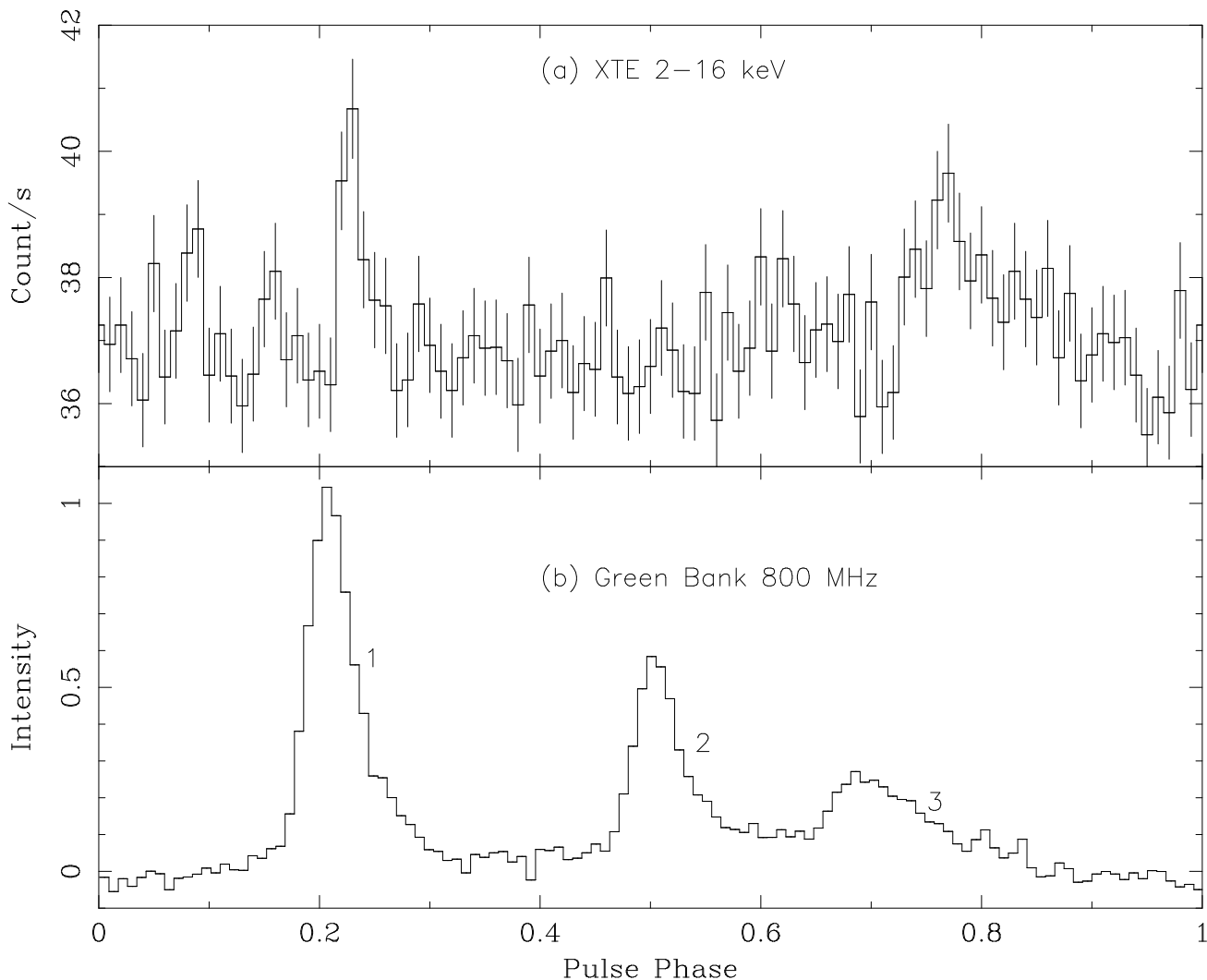


FIG. 2.—PSR B1821–24. Light curves based on (a) *RXTE* PCA (2–16 keV), and (b) Green Bank radio (800 MHz) observations, using timing ephemeris B1821–24G. The *RXTE* light curve is labeled in counts per second per bin (at 100 bins per period) with 1σ errors indicated. The radio pulse components are identified by means of the same numbering as Backer & Sallmen (1997).

tainty in the dispersion measure. We have summarized the phases of the pulse component peaks in Table 2. The quoted errors are approximate 1σ values. One should note that the difference between the pulse profiles derived from the Jodrell Bank and Green Bank observations, as shown in Figures 1 and 2, is due in part to the difference in temporal resolution, but also in part to the difference in observing frequency. The spectral characteristics of the two components are very different at radio frequencies: at higher frequencies pulse component 2 is generally stronger than pulse component 1. The high-resolution pulse profile at 1395 MHz presented by Backer & Sallmen (1997) provides an easier comparison.

It is interesting to note that, after the Crab pulsar, we have here once again a pulsar where the main radio and X-ray pulse component peaks are coincident to better than 20 milliperiods.

This public *RXTE* observation only yielded 6559 s of exposure. Two of us (Y. S. and N. K.) have obtained a proprietary observation of much longer duration. It seems prudent, therefore, to defer discussion of other characteristics, such as spectral properties, to the publication of those observations.

5. PSR B1509–58

The timing data for PSR B1509–58 were obtained by means of the Parkes telescope⁹ in a continuation of the observational program described by Kaspi et al. (1994); the observing frequency was 1400 MHz, the assumed dispersion measure 253.2 pc cm^{-3} . The radio pulse profile displays a single pulse component with a full width at half-power of about 0.1 period; the phase is referenced to the peak of that pulse with an accuracy of about 1 ms. The timing ephemeris is provided in Table 1.

5.1. Timing Analysis

In X-rays, this pulsar has been monitored during the entire *RXTE* mission to date. The monitoring observations each lasted at least 2000 s and were done approximately once a month. Figure 3 shows the light curves in the 2–16 keV PCA band for 10 of these observations. The vertical

⁹ The Parkes telescope is part of the Australia Telescope, which is funded by the Commonwealth of Australia for operation as a National Facility by CSIRO.

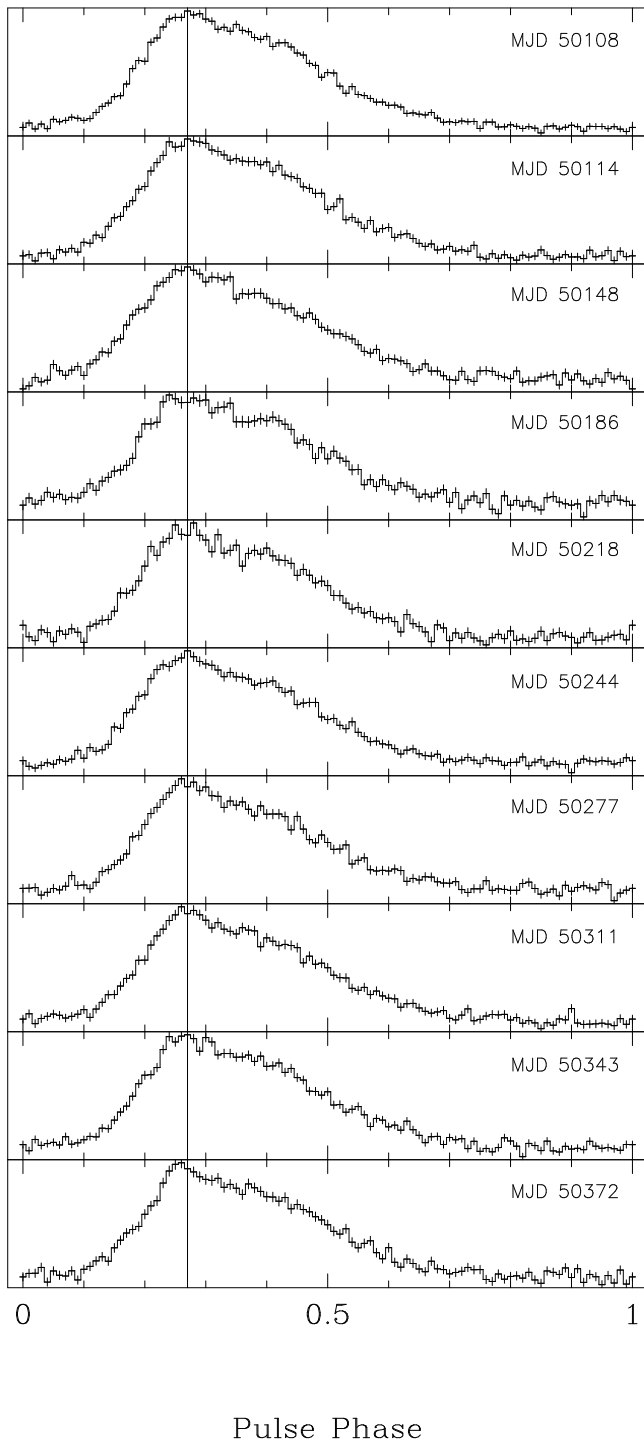


FIG. 3.—PSR B1509—58. Light curves for 10 epochs (PCA 2–16 keV). The error bars represent 1σ errors. The vertical line indicates phase 0.27.

line is drawn at phase 0.27. There are clearly variations in these light curves, but they are consistent with a constant (X-ray radio) peak phase lag of 0.27 ± 0.01 period, as indicated by the distribution, in phase, of the peak bins of the 10 light curves. We have also analyzed the cross correlation functions between the 10 light curves. The centroids are all distributed within 0.008 of the average. From this we conclude that the variation in phase is no more than 0.005 period, comparable to the uncertainty in the radio timing

ephemeris. As a matter of fact, there appear to be systematic variations at this level that are correlated with the different timing ephemeris entries. Our phase lag result is consistent with the phase lag derived by Kawai et al. (1991), but is different from that determined by Ulmer et al. (1993). We will return to this issue in the discussion section, below. The shapes of the light curves agree with those obtained by both previous investigations.

Figure 4 shows the accumulated light curves for the bands 2–4, 4–8, 8–16, 16–32, 32–64, 64–128 keV (the first

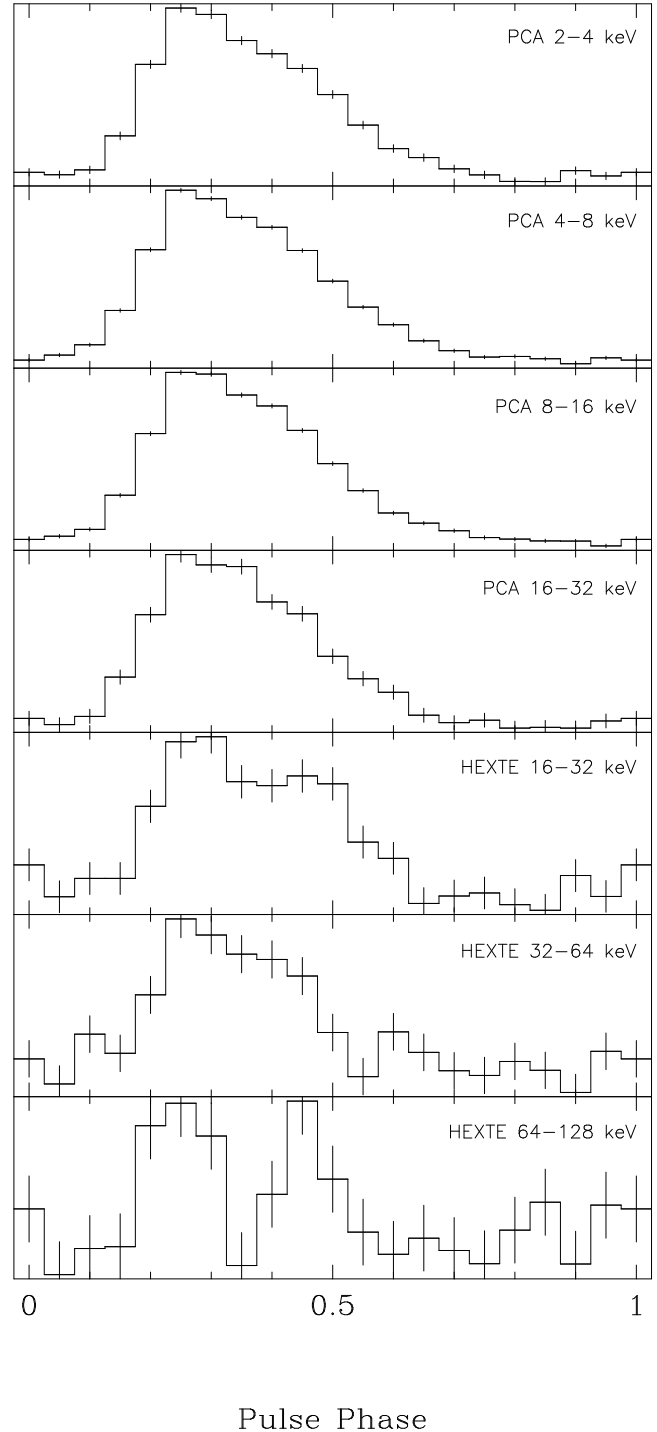


FIG. 4.—PSR B1509—58. Accumulated light curves for seven energy bands. The vertical scale is arbitrary; the error bars represent 1σ errors.

four PCA, the last three HEXTE). These data are consistent with a phase lag of 0.27, independent of energy. Note that the changes in pulse profile with energy are probably not significant, as indicated by the spectral analysis, below.

5.2. Spectral Analysis

We performed phase-resolved spectral analysis, using the program XSPEC. For this purpose we accumulated PCA and HEXTE spectra in eight slices of 0.05 period, from phase 0.20 through phase 0.55. The average count rate spectrum in the phase range from 0.7 through 1.1 was used as the value for the unpulsed components of internal and cosmic background, as well as the source itself, and subtracted from spectra of the pulsed radiation. It transpired that the spectra could all be fitted well with a simple power-law model with interstellar absorption (Morrison & McCammon 1983). On the basis of fits to spectra near the peak of the pulse, we adopted a value for N_{H} of 6×10^{22} . Hence, only photon spectral index and total flux were allowed to vary. The somewhat surprising result is that all spectra are consistent with a single value for the photon index: 1.345 ± 0.010 ; i.e., the photon flux density (photons $\text{cm}^{-2} \text{s}^{-1} \text{keV}^{-1}$) is proportional to $E^{-1.345 \pm 0.01}$. The derived photon index values, with formal errors and reduced χ^2 , are listed in Table 3. Figure 5 presents the spectral fit for phase 0.25. It is illustrative of the fits at other pulse phases.

TABLE 3
PSR B1509L — 58 FITTED PHOTON INDEX AS A
FUNCTION OF PHASE

Phase	Net Count Rate	Photon Index	Error	Reduced χ^2
0.20.....	29.2	1.389	0.027	0.909
0.25.....	45.2	1.356	0.018	1.097
0.30.....	43.4	1.341	0.018	1.050
0.35.....	37.6	1.343	0.021	1.021
0.40.....	34.5	1.342	0.022	1.081
0.45.....	29.0	1.341	0.026	0.861
0.50.....	20.3	1.419	0.037	1.261
0.55.....	12.8	1.397	0.056	0.838

The value for the photon index of 1.345 is consistent with the one obtained by Kawai, Okayasu, & Sekimoto (1993). They found 1.30 ± 0.05 . Matz et al. (1994) determined the index to be 1.68 ± 0.09 for the energy range 50 keV–5 MeV based on OSSE observations and speculated that there has to be a break in the spectrum between 20 and 80 keV. A broken power-law fit to our spectra does not improve the fit. Hence, we conclude that the break is most likely to occur above 50 keV. A more comprehensive spectral analysis has been presented by Marsden et al. (1997).

The surprise lies in the fact that there is no significant change of photon index with phase. Kawai et al. (1991) have

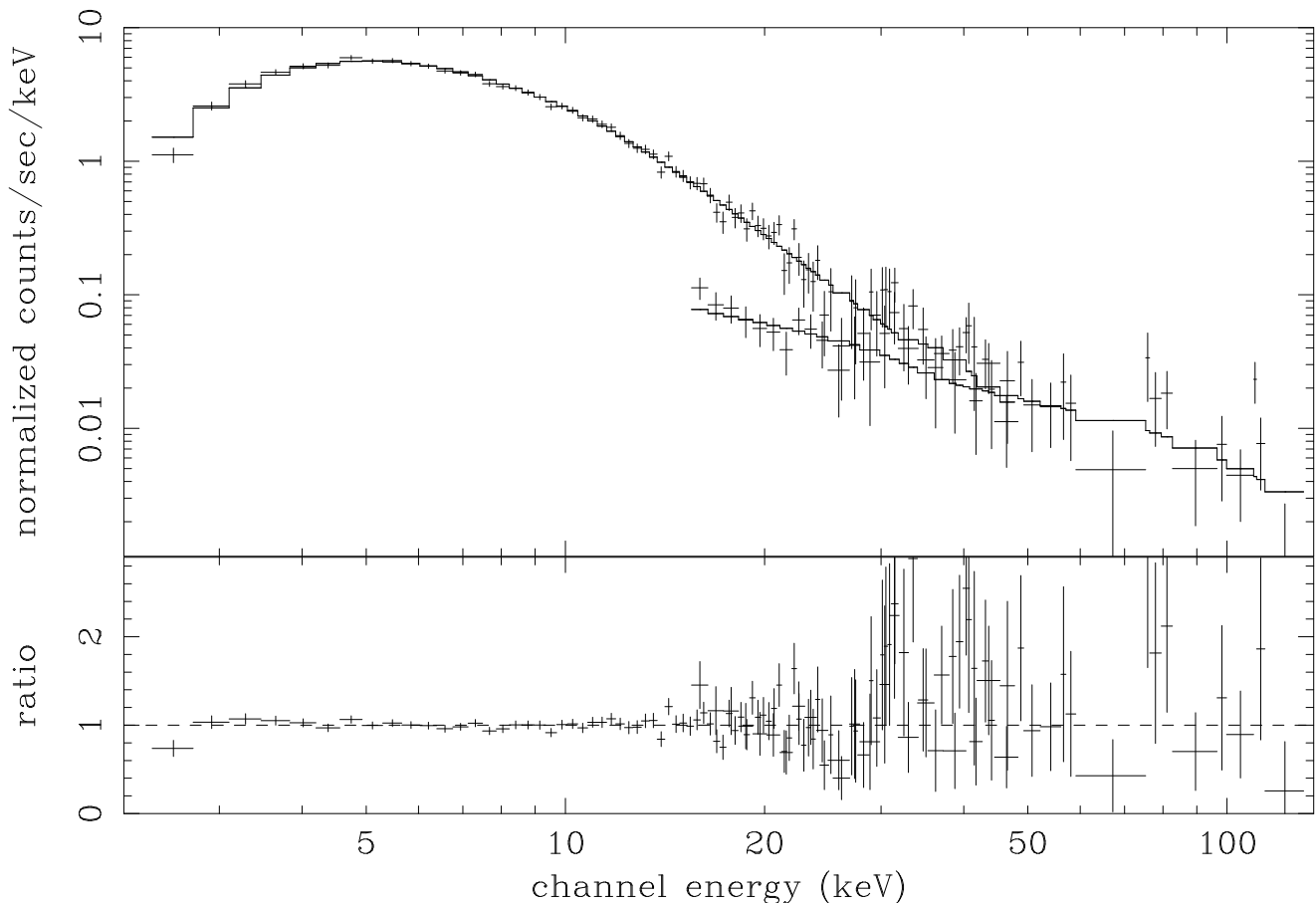


FIG. 5.—PSR B1509—58. Spectral fit for pulse phase 0.25. The crosses (1σ error bars) in the upper panel represent the observations, the solid lines the model convolved with the response matrices. The left-hand segment pertains to PCA data, the right-hand segment to HEXTE data. The lower panel presents the ratio data/model.

speculated that there may be two components making up PSR B1509–58's X-ray pulse shape. The light curves seem to support this notion. But if such is the case, then the two components are, at least to *RXTE*, spectrally indistinguishable.

5.3. Discussion

The significance of our results for the difference in phase lag between this paper and Kawai et al. (1991) on the one hand and Ulmer et al. (1993) on the other is considerable. Kawai et al. (1991) find a value of 0.25 ± 0.02 for the 2–11 keV band, which is consistent with the value we find of 0.27 ± 0.01 for the 2–16 keV band. This phase lag refers explicitly to the peak. Ulmer et al. (1993) find (fitting to the shape of the Kawai et al. 1991 light curve) a phase lag of 0.32 ± 0.02 for BATSE data covering the band 20–400 keV (the OSSE observation is less relevant in this context). We should also mention, at this point, the results from the balloon experiment “Welcome,” reported by Gunji et al. (1994). Covering the range 94–240 keV, these observations are consistent both spectrally and temporarily with the *Ginga* data; the uncertainties preclude a stronger statement. The inconsistency with the Ulmer et al. (1993) result (8 ms) is especially troubling because the *CGRO* absolute time information is qualitatively much better than that of the other missions. It cannot be summarily dismissed as a *CGRO* clock or software error since such would have had very noticeable effects on, for instance, the Crab pulsar light curves from *CGRO* instruments.

We attempted to resolve the issue by reprocessing 5 yr of BATSE observations of PSR B1509–58 from the public *CGRO* archive, using all data at energies higher than 32 keV. The result is shown in Figure 6. Cross correlation analysis of the pulse profiles reveals that the BATSE light curve is shifted by 0.03 period, or 5 ms. Although this difference is smaller than for the result of Ulmer et al. (1993), it still exceeds the acceptable bounds, it is still too large to be unnoticed in the Crab data, and it raises the question why this BATSE time lag is different from what was found previously. There are only two explanations possible that can reconcile the results of the three space-based investigations (Kawai et al. 1991; Ulmer et al. 1993; and the present paper): the phase lag varies with energy, or the phase lag varies in time.

Energy dependence seemed unlikely, judging from the full energy range of the BATSE and OSSE observations of Ulmer et al. (1993), but remained possible. Our data show convincingly that there is no variation of phase lag over the range 2–100 keV. Even if the reader may not be persuaded by Figure 4 that this statement applies above 50 keV, the hypothesis requires a considerable hardening of the spectrum at phases above 0.30; this is clearly ruled out by our spectral analysis. This is corroborated by the combination of *Ginga* and Welcome observations by Kawai et al. (1991) and Gunji et al. (1994), which make it seem very unlikely that a break in the spectrum would occur below 100 keV.

Time evolution of the phase lag was all but ruled out by Ulmer et al. (1993), on the basis of their BATSE and OSSE observations. This is corroborated by our data, at least on timescales of 1 yr or less (Fig. 3). It is also worth mentioning that the radio ephemerides were created over short durations so that phase drift due to low-level timing noise observed in the pulsar cannot be the cause of the discrepancy.

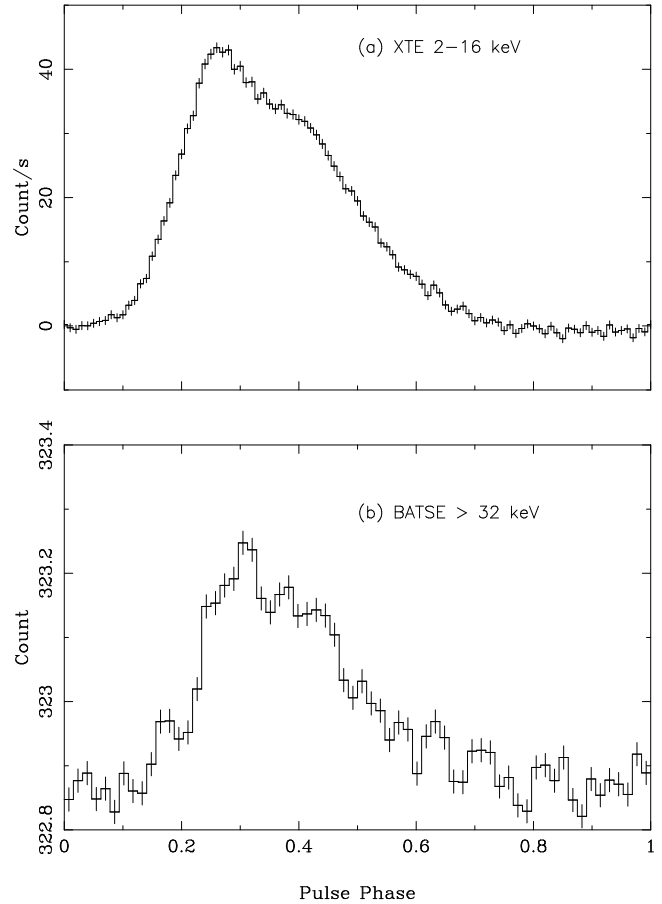


FIG. 6.—PSR B1509–58. Accumulated light curves based on (a) *RXTE* PCA (2–16 keV) and (b) BATSE (> 32 keV) observations. The error bars represent 1 σ errors.

A change in the pulsar dispersion measure would result in an apparent change in phase offset between radio and X-ray energies. However, the dispersion measure change required to explain the discrepancy is over an order of magnitude larger than is expected based on similar results for most other pulsars (Backer et al. 1993, and references therein); it requires an increase of more than $0.5 \text{ pc cm}^{-3} \text{ yr}^{-1}$. In our analysis we have used the value for the dispersion measure of $253.2 \pm 1.9 \text{ pc cm}^{-3}$ given by Kaspi et al. (1994). This same value was used by all investigators quoted in the present paper. Recently (MJD 50,780–50,784), one of us (R. N. M.) made a new measurement of the dispersion measure and obtained a value of $255.3 \pm 0.3 \text{ pc cm}^{-3}$ (2σ error). A preliminary analysis of nearly contemporaneous *RXTE* observations, using this new value, yields a phase offset of 0.29 ± 0.01 . At first glance, this appears to resolve the inconsistency, and it very well may, but one has to be extremely careful: the two determinations of the dispersion measure are still marginally consistent with each other, and there is no irrefutable evidence that the dispersion measure actually changed. If we just take the extremes as indicated by the quoted errors, the change in dispersion measure over 7 yr may have been anywhere between 0 and 4 pc cm^{-3} .

In conclusion, we note that a gradual change in dispersion measure from 253.2 pc cm^{-3} in 1990 to 255.3 pc cm^{-3} in 1997 would explain the changes in phase lag. But the plausibility of such a scenario needs to be confirmed by future monitoring of the dispersion measure.

Support for one of us (V. M. K.) was provided by Hubble Fellowship grant number HF-1061.01-94A from the Space Telescope Science Institute, which is operated by the

Association of Universities for Research in Astronomy, Inc., under NASA contract NAS 5-26555. We are grateful to an anonymous referee for helpful comments.

REFERENCES

- Backer, D. C., Hama, S., Van Hook, S., & Foster, R. S. 1993, *ApJ*, 404, 636
 Backer, D. C., & Sallmen, S. 1997, *AJ*, 114, 1539
 Buccheri, R., et al. 1978, *A&A*, 69, 141
 Cheng, K. S., Ho, C., & Ruderman, M. A. 1986, *ApJ*, 300, 522
 Daugherty, J. K., & Harding, A. K. 1982, *ApJ*, 252, 337
 Gunji, S., et al. 1994, *ApJ*, 428, 284
 Kanbach, G., et al. 1994, *A&A*, 289, 855
 Kaspi, V. M., Manchester, R. N., Siegman, B., Johnston, S., & Lyne, A. G. 1994, *ApJ*, 422, L83
 Kawai, N., Okayasu, R., Brinkmann, W., Manchester, R., Lyne, A. G., & D'Amico, N. 1991, *ApJ*, 383, L65
 Kawai, N., Okayasu, R., & Sekimoto, Y. 1993, in *AIP Conf. Proc.* 280, *Compton Gamma-Ray Observatory*, ed. M. Friedlander, N. Gehrels, & D. J. Macomb (New York: AIP), 204
 Marsden, D., et al. 1997, *ApJ*, 491, L39
 Masnou, J. L., et al. 1994, *A&A*, 290, 503
 Matz, S. M., et al. 1994, *ApJ*, 434, 288
 Morrison, R., & McCammon, D. 1983, *ApJ*, 270, 119
 NASA/GSFC. 1991, *Users Spacecraft Clock Calibration System (USCCS) User's Guide (531-TR-001)* (Greenbelt: NASA/GSFC)
 Nolan, P. L., et al. 1993, *ApJ*, 409, 697
 Romani, R. W., & Yadigaroglu, I.-A. 1995, *ApJ*, 438, 314
 Rots, A. H., et al. 1998a, in *Neutron Stars and Pulsars*, ed. S. Shibata (Tokyo: Universal Academy Press), in press
 Rots, A. H., Jahoda, K., Lyne, A. G., Morgan, E. H., & Strohmayer, T. 1998b, in preparation
 Saito, Y., Kawai, N., Kamae, T., Shibata, S., Dotani, T., & Kulkarni, S. R. 1997a, *ApJ*, 477, L37
 Saito, Y., et al. 1997b, *ASCANEWS* (Greenbelt: GSFC/HEASARC), No. 5, 34
 Seidelmann, P. K., Guinot, B., & Doggett, L. E. 1992, *Explanatory Supplement to the Astronomical Almanac*, ed. P. K. Seidelmann (Mill Valley: University Science Books), 39
 Smith, F. G. 1986, *MNRAS*, 219, 729
 Standish, E. M. 1982, *A&A*, 114, 297
 ———. 1990, *A&A*, 233, 252
 Ulmer, M. P., et al. 1993, *ApJ*, 417, 738
 ———. 1994, *ApJ*, 432, 228